scientific reports

Check for updates

OPEN

Enhanced antibody responses in CD19-Cre mice

Diogo M. Cunha[1,2,3,5], Sara Hernández-Pérez[1,2,3,4,5] & Pieta K. Mattila[1,2,3]✉

CD19-Cre is an important and widely used Cre-lox model for B cell-specific genetic manipulation in murine systems. Mice carrying one allele of CD19-Cre are, at the same time, rendered heterozygote for CD19, a crucial coreceptor of the B cell antigen receptor (BCR). As a result, CD19-Cre mice exhibit diminished expression levels of CD19, with potential, yet insufficiently examined, consequences in B cell activation. Here, we report significantly heightened antibody responses upon both T-dependent (NP-KLH) and T-independent (NP-Ficoll) immunizations as well as elevated levels of basal IgM immunoglobulin levels in CD19-Cre mice. In vitro, we observed enhanced class-switch recombination and a moderate reduction in B cell proliferation upon LPS and IFNγ stimulation, yet no drastic differences in BCR signalling. Our findings warrant careful consideration in the use of CD19-Cre mouse model in B cell research.

Keywords B cells, BCR, CD19, Antibody response, Class-switch recombination

The Cre-lox system is an extensively used tool in genetic engineering to create tissue-specific gene knockout (KO) or knockin models. The system relies on the expression of the Cre recombinase enzyme that mediates site-specific recombination between DNA sequences flanked by loxP sites (referred to as 'floxed'). This enables precise manipulation of gene expression in specific tissues or developmental stages, depending on the exact promoter region under which Cre-encoding cDNA is integrated in the genome. Notewhorthy Cre-lox models for B cell-specific genetic targeting in mice include Mb1-Cre, CD19-Cre, and CD21-Cre models, where Cre expression is driven by the Mb1, Cd19, or CD21 promoters, respectively[1–3]. As every model have distinct cell stage specificities and recombination efficiencies, the choice of the model ultimately depends on the research question and on the availability of the specific Cre-lines. For instance, the Mb1-Cre model leads to Cre expression at very early pro-B cell stage and CD19-Cre later in the pre-B cell stage of B cell development, while CD21-Cre is expressed in mature B cells as well as in follicular dendritic cells[4].

CD19-Cre mouse model has been widely adopted in B cell research. Over the years, this model has been extensively used to generate B cell-specific gene KO strains, to investigate the effect of such genes in B cell development and function, immune responses to pathogens, or autoimmune diseases[5,6]. The main largely acknowledged limitation for the CD19-Cre model has been its relatively poor Cre-recombination efficiency[7]. However, there is a second limitation to this system: in the CD19-Cre model, as for other Cre models, the Cre-cassette is strategically positioned near the gene promoter region. Importantly, this obstructs the transcription of the endogenous Cd19 allele, resulting in hypomorphic expression of CD19 in the heterozygoes ($CD19^{WT/Cre}$) animals typically used in the conditional KO-models[8,9]. This feature has also been exploited to explore the CD19-KO phenotype using homozygous ($CD19^{Cre/Cre}$) mice[8,10].

Despite the widespread use of the CD19-Cre model in B cell research, the potential impact caused by the hypomorphic CD19 expression in B cells in these mice has not been adequately assessed. CD19 is an important BCR co-receptor, expressed early in B cell development. Enabled by its B cell-specific expression pattern, it also serves as one of the most widely used B cell lineage markers. Loss of CD19 expression in mice, or mutations in CD19 in humans have been associated with immuno deficiencies[11], and augmented levels of CD19 with autoimmunity[12–16]. Interestingly, CD19-deficient B cells react robustly to soluble antigen stimulation, but their activation by surface-tethered antigens, inducing the formation of the immune synapse, is compromised[8,10]. CD19 also plays a pivotal role in antigen-independent triggering of the BCR upon destabilization of the cortical filamentous actin network[8,17]. Given the significance of CD19 as a co-receptor crucial for B cell function, it becomes imperative to assess whether the diminished CD19 levels in CD19-Cre model have functional implications in B cells. Alarmingly, Zhao et al. recently reported increased antibody responses in CD19-Cre

[1]Institute of Biomedicine and MediCity Research Laboratories, University of Turku, Turku, Finland. [2]InFLAMES Research Flagship, University of Turku, Turku, Finland. [3]Turku Bioscience, University of Turku and Åbo Akademi University, Turku, Finland. [4]Institute of Immunity and Transplantation (IIT), Division of Infection and Immunity, University College London, London, UK. [5]Diogo M. Cunha and Sara Hernández-Pérez contributed equally. ✉email: pieta.mattila@utu.fi

animals upon immunization with the T-dependent (TD) antigen NP-OVA and the T-independent (TI) antigen NP-Ficoll[9]. In this work, we have validated these provokative findings in our $CD19^{WT/Cre}$ mice. Additionally, we report augmented basal IgM levels in these mice as well as reveal altered in vitro activation characteristics in $CD19^{WT/Cre}$ B cells. These results urge for careful consideration in the use of CD19-Cre in B cell research.

Results

First, to verify the hypomorphic expression of CD19 in CD19-Cre mice, we stained the splenic B cells from CD19-Cre mice and their CD19-WT littermates ($CD19^{WT/WT}$) for surface CD19 and analysed by flow cytometry. We detected approximately 50% reduction in the levels of CD19 in $CD19^{WT/Cre}$ animals (Fig. 1A). IgM and IgD BCR levels, on the other hand, were unaltered. Next, we assessed the basal antibody levels and found increased levels of IgM antibodies in $CD19^{WT/Cre}$ mice, while the other isotypes did not show significantly altered titers (Fig. 1B). To investigate the antibody responses in these animals, we immunised a cohort of $CD19^{WT/Cre}$ and $CD19^{WT/WT}$ mice with NP-KLH (TD immunization) in the presence of alum, and another cohort with NP-Ficoll (TI immunization) and monitored the levels of IgG subtypes and IgM for four weeks. Our findings, in line with the previous study employing NP-OVA and NP-Ficoll[9], revealed an overall heightened response to immunization in $CD19^{WT/Cre}$ mice (Fig. 1C, D). We saw increase both in IgM responses, as well as in IgG with more pronounced effects in isotypes IgG2c and IgG3. These observations are particularly intriguing because CD19 is recognized for its role rather in boosting BCR signalling, particularly via PI3K through an interaction with the p85α PI3K regulatory subunit[18]. Also, $CD19^{Cre/Cre}$ mice have been reported with abnormal B cell numbers and a profound reduction in TD immunisation-induced antibodies[12,14,19].

To gain insight into the possible mechanisms underlying the hyperactive immunization phenotype, we performed in vitro experiments for BCR signalling and immunoglobulin class-switch recombination (CSR) with isolated $CD19^{WT/WT}$ and $CD19^{WT/Cre}$ mouse splenic B cells. First, we analysed CSR upon different stimulatory conditions and found significantly increased CSR activity in $CD19^{WT/Cre}$ cells. CSR into IgG1 was increased in several conditions known to induce IgG1 expression, and increased switching to IgG2c expression was found upon induction with IFNγ (Fig. 2A). In addition to the observed changes in CSR towards IgG1 and IgG2c, $CD19^{WT/Cre}$ cells showed a moderate reduction in proliferation following stimulation with LPS and IFNγ indicated by a significant decrease in the division and expansion capability of these cells compared to $CD19^{WT/WT}$ B cells (Fig. 2B). With other stimuli tested, there were no changes observed in B cell proliferation.

Next, resting splenic B cells isolated from $CD19^{WT/WT}$ and $CD19^{WT/Cre}$ mice were activated with surrogate antigen for 15 min and analysed for downstream signaling using intracellular immunostainings by flow cytometry. The only significant alteration observed was reduced fold-change in PI3K phosphorylation upon cell activation, which resulted from mildly increased basal levels and lowered activation-induced levels (Fig. 3A). While consistent with the literature, this effect was very small and we did not observe significant reduction in the pS6, considered to be downstream of PI3K. PI3K is deemed one of the main pathways positively regulated by phosphorylation of CD19[20]. However, PI3K can also be activated by CD19-independent means upon BCR signaling as the PI3K-deficient cells feature more severe signaling defects than cells where CD19 is, via mutagenesis, rendered unable to recruit PI3K[8,18]. Curiously, $CD19^{Cre/Cre}$ B cells have been shown to be able to activate Akt, the main target dowstream of PI3K, even to higher extent than WT cells, upon soluble surrogate antigen stimulation[8], although CD19 is critically required for B cell activation by surface-bound antigens[10]. These examples, as well as our results on $CD19^{WT/Cre}$ mice and cells, hypomorphic in CD19, demonstrate the highly context-dependent nature of CD19 function, the molecular mechanisms of which still remain ill-understood.

Finally, we asked the question if the hightened IgM levels could be explained by increased propensity of MZ or peritoneal B1a cells to respond to BCR activation. For this, we isolated, from $CD19^{WT/WT}$ and $CD19^{WT/Cre}$ mice, splenocytes and perintoneal cells for examination of marginal zone (MZ) and peritoneal B1a B cells, respectively. The cells were activated with anti-IgM, stained for extracellular markers to gate on the defined cell populations, and then fixed and permeabilized for probing of phospho-proteins. Due to technical challenges in perserving both the extracellular markers and intracellular phospho-protein detection, we were restricted with phospho-BTK and phospho-Plcγ2 as the stainings of the other phospho-proteins did not yield reliable results. Of note, due to the loss of IgM staining following sample permeabilization, the gate for MZ population (Supplementary Fig. 1) included also IgM^- cells, however, those cells represent a minority in this gate[22] and would not react to the IgM-mediated activation. Our results did not reveal any significant changes between $CD19^{WT/WT}$ and $CD19^{WT/Cre}$ MZ or B1a cells, although the $CD19^{WT/Cre}$ cells showed a tendency for slightly higher levels of both the phospho-BTK and phospho-Plcγ2 both in resting and activated state (Supplementary Fig. 2). Together, our data suggest no major augmentation in the signaling mediated solely by the BCR, but rather in combinatorial settings, as evidenced by the enhanced CSR (Fig. 2).

Discussion

Our findings highlight an important, unnoticed drawback of the CD19-Cre model, widely used in immunological research, and shed light on the complex relationship between CD19 and antibody responses. Using TD and TI immunization models—NP-KLH and NP-Ficoll, respectively—and measuring basal antibody titers, we show that the inactivation of the Cd19 allele with the Cre cassette can enhance humoral immunity. We also found increased in vitro CSR activity in isolated splenic $CD19^{Cre/WT}$ B cells. These phenotypes are likely a result of the hypomorphic CD19 expression levels in $CD19^{Cre/WT}$ B cells; however, the exact molecular mechanism remains unclear.

Our results strongly support the recent report by Zhao and colleagues, who showed increased antibody levels in $CD19^{Cre/WT}$ mice upon TD immunization with NP-OVA and TI immunization with NP-Ficoll, as well as enhanced antibody secretion *in vitro*[9]. Additionally, Zhao and colleagues reported decreased marginal zone B

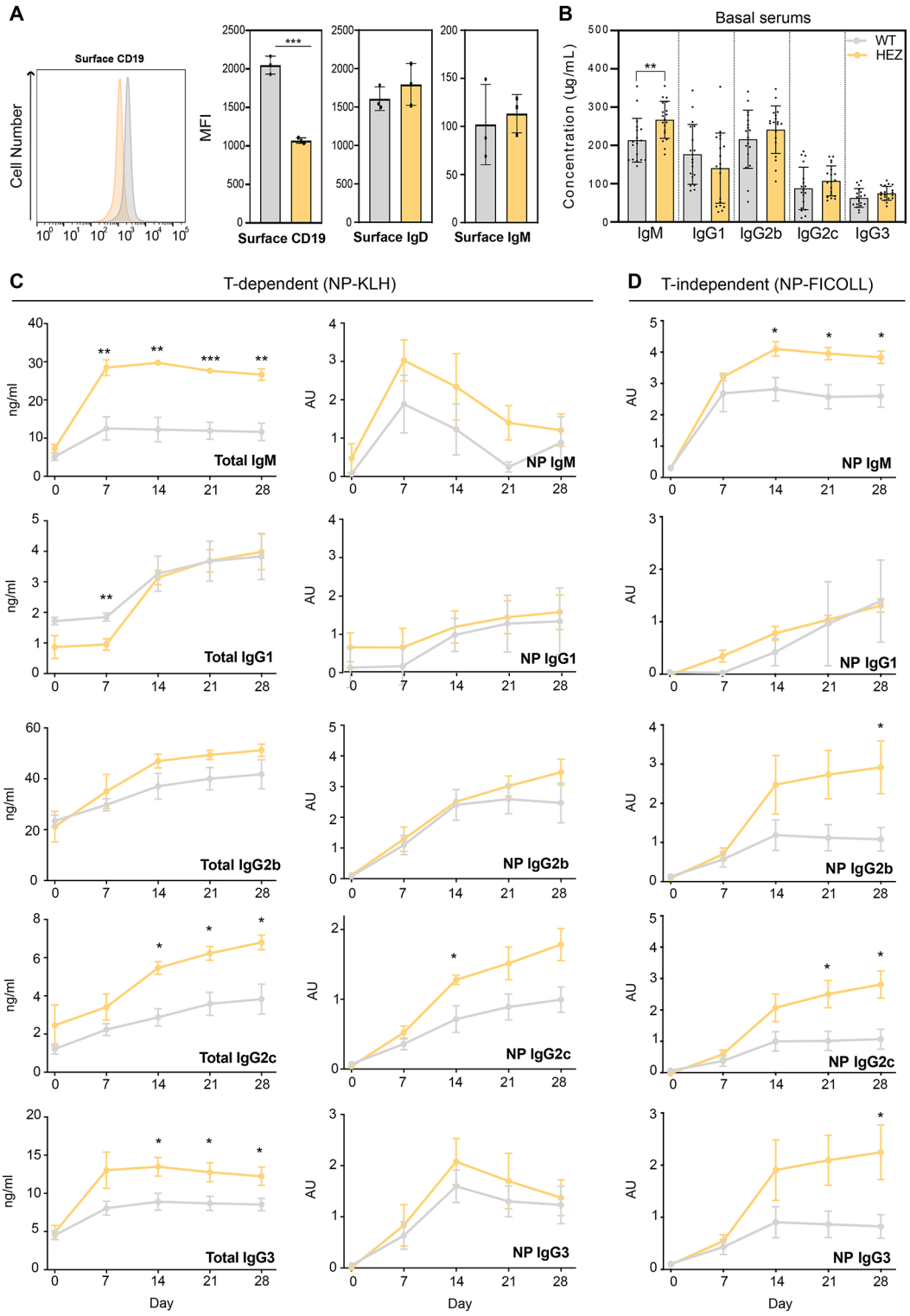

Fig. 1. Increased antibody responses in CD19$^{Cre/WT}$ mice. (**A**) Surface CD19, IgD and IgM levels in primary B cells isolated from CD19$^{WT/WT}$ (grey) and CD19$^{Cre/WT}$ (yellow) mice, assessed by flow cytometry. (**B**) Basal antibody levels, prior to immunisation, in CD19$^{WT/WT}$ and CD19$^{Cre/WT}$ animals assessed from the sera of the mice by ELISA (n > 10 mice). (**C**) Total and NP-specific (NP20) levels of antibodies after NP-KLH-alum immunisation in CD19$^{WT/WT}$ (grey) and CD19$^{Cre/WT}$ (yellow) mice (n = 4 mice of each genotype). (**D**) NP-specific levels (NP20) after NP-Ficoll immunisation (n = 4 mice of each genotype). Unpaired Student's t-test: $^{*}P < 0.05$, $^{**}P < 0.01$, $^{***}P < 0.001$.

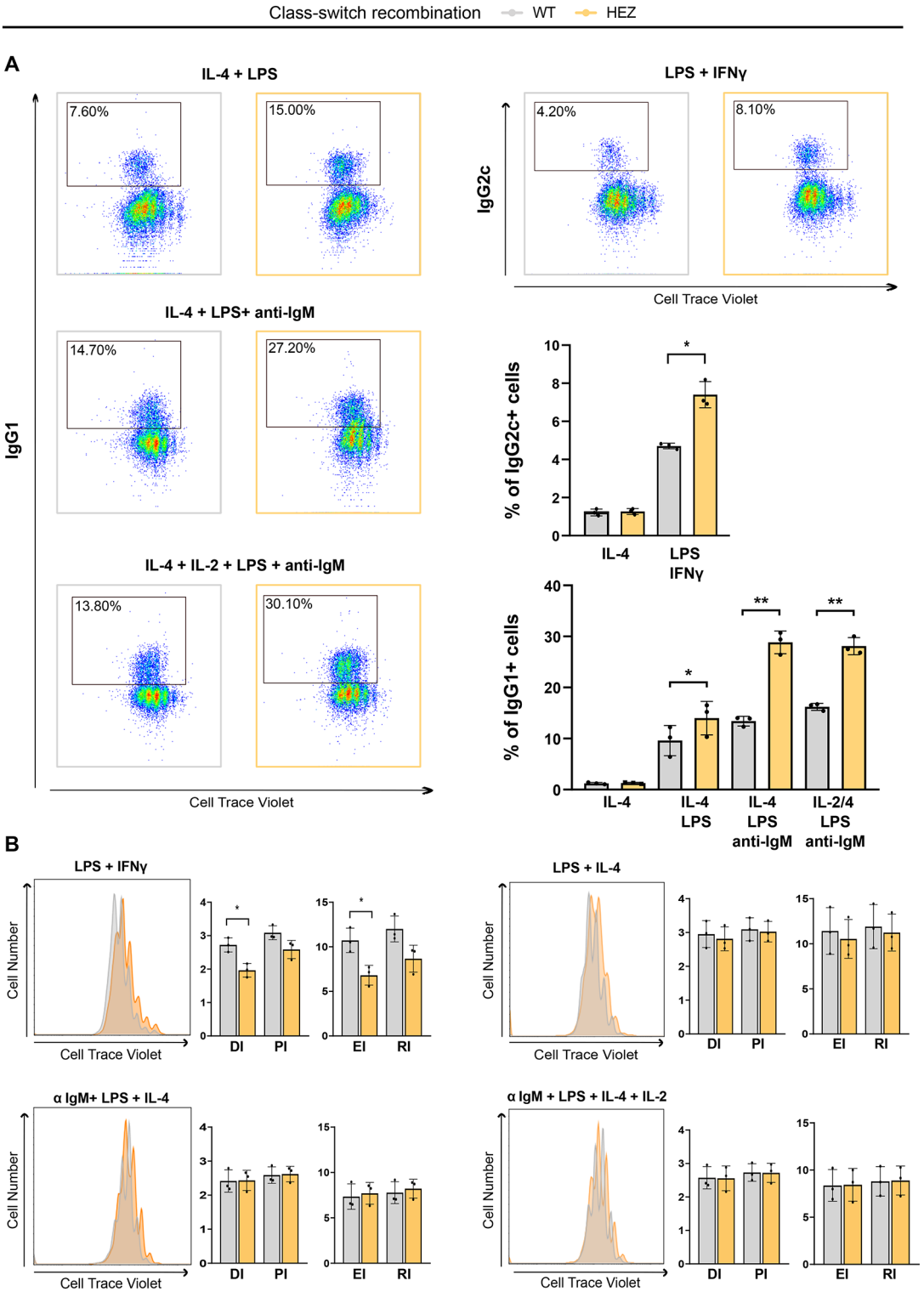

Fig. 2. Increased class-switch recombination activity in CD19$^{Cre/WT}$ B cells. (**A**) Mouse primary B cells isolated from CD19$^{WT/WT}$ (grey) and CD19$^{Cre/WT}$ (yellow) mice were analysed for BCR class-switch (IgG1 + , IgG2c +) in response to different stimuli after 3 days. Data are shown as representative flow cytometry plots and analysis of percentage of cells (mean ± SD) from three independent experiments. (**B**) Proliferation of Cell Trace Violet (CTV)-labeled primary B cells isolated from CD19$^{WT/WT}$ (grey) and CD19$^{Cre/WT}$ (yellow) mice was analyzed by flow cytometry from cells cultured for 3 days in the presence of LPS supplemented with IFNγ; IL-4; IL-4 + anti-IgM; or IL-4 + anti-IgM + IL-2. Representative histograms of 3 independent experiments are shown together with analysis of division index (DI), proliferation index (PI), expansion index (EI) and replication index (RI), calculated in FlowJo platform and presented as bar graphs. Paired Student's t-test: $^{*}P < 0.05$, $^{**}P < 0.01$.

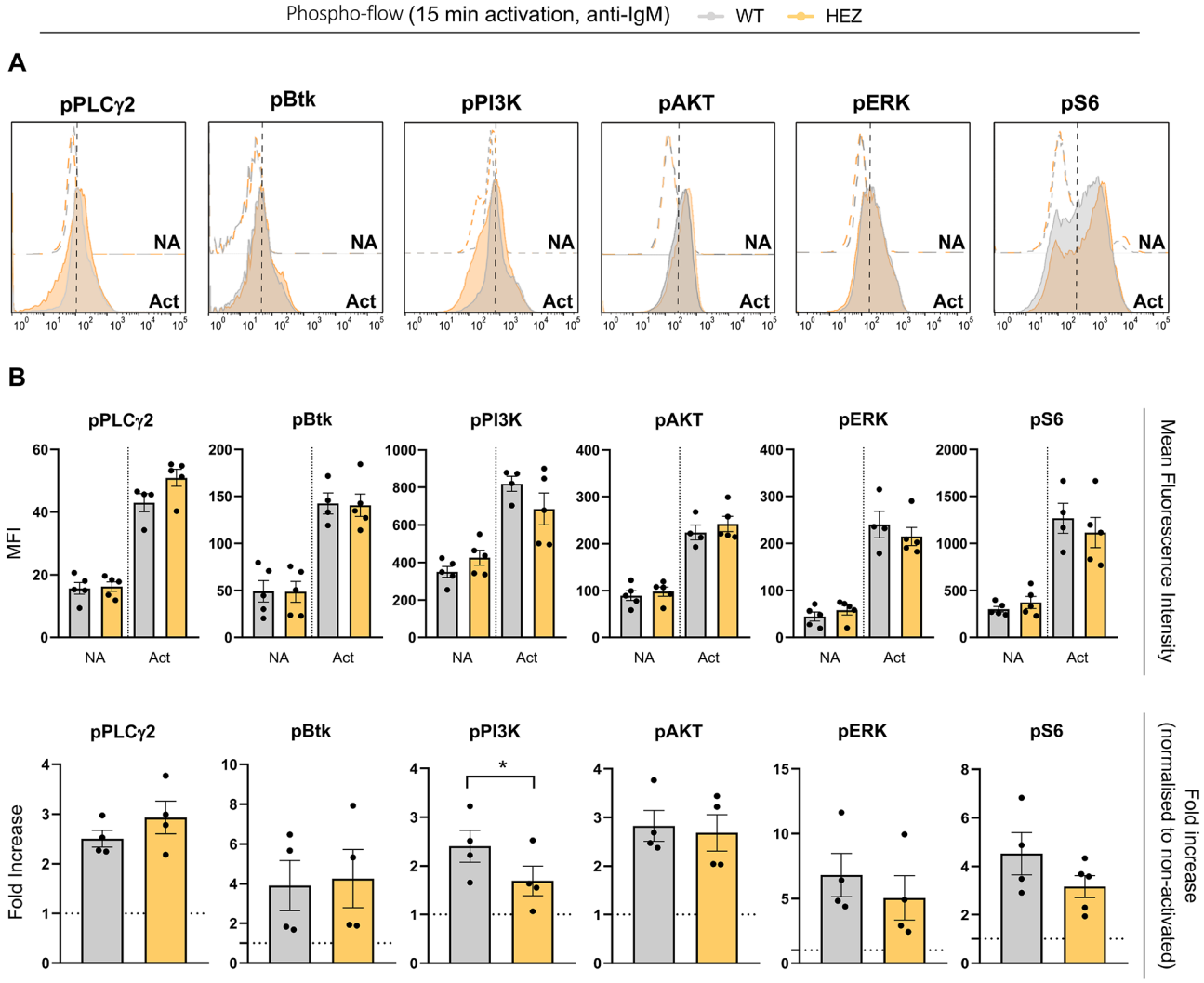

Fig. 3. $CD19^{Cre/WT}$ B cells respond by normal phosphorylation kinetics to BCR engagement. Analysis of BCR signalling by phospho-flow. Cells were activated with 10 µg/ml of $F(ab')_2$ anti-IgM in solution for 15 min and then fixed and stained with the phosphorylation-specific antibodies. (**A**) Upper histograms represent the intensity of the phosphorylation-specific antibodies in non-activated (NA) $CD19^{WT/WT}$ (grey dotted line) and $CD19^{Cre/WT}$ (yellow dotted line) B cells. Lower histograms represent the intensity of the phosphorylation-specific antibodies in activated (Act) $CD19^{WT/WT}$ (grey, filled) and $CD19^{Cre/WT}$ (yellow, filled) B cells. Representative histograms of 4 independent experiments are shown. (**B**) Mean Fluorescence Intensity (MFI) of the phosphorylation-specific antibody signals in non-activated and activated conditions (upper row) and the fold increase upon activation (lower row) in $CD19^{WT/WT}$ (grey) and $CD19^{Cre/WT}$ (yellow) B cells, represented as bar graphs. Horizontal dotted line at the value 1 in fold change graphs represents the level of non-activated conditions. Paired Student's t-test: $^*P < 0.05$.

cells numbers, but did not detect changes in CSR into $IgG1^+$ B cells or plasma cell, in vitro, while our resuls show a clear increase in the CSR into $IgG1^+$ and also IgG2c. The difference between our work and Zhao et al. could result from the addition of BCR agonist that in our experiments increased CSR notably, while the conditions of LPS + IL4, also used by Zhao et al., only lead into a modest increase of CSR in CD19-Cre cells. This also directed us to examine the BCR-mediated signaling reponses, which Zhao et al., did not include in their study at all. However we did not detect significant changes in the BCR-mediated signaling, as tested in follicular, MZ, and B1a B cells. These results suggest that the enhanced antibody responses and CSR seen in CD19-cre B cells would be a result of more complex signaling environment, and underlines the need for better understanding of the function of CD19 beyond its role as a BCR co-receptor. Together, our results disclose clear alterations of B cell function induced by the CD19-Cre allele, potentially confounding results obtained by using this experimental model.

The until now poor recognition of the altered phenotype of $CD19^{Cre/WT}$ mice can be explained by many studies simply not including both $CD19^{Cre/WT}$ and $CD19^{WT/WT}$ controls. Also these controls are not always shown in the articles, even if that would be reported in the text, which hinders re-assesment of the data. Zhao et

al., performed a comprehensive literature review analysing 256 articles using the CD19-Cre model[9]. 56 articles were noted to compare $CD19^{Cre/WT}$ mice with $CD19^{WT/WT}$. 50% of these (28 publications) reported reduced MZB/B1a cells and/or higher antibody levels in sera or culture supernatants. On the other hand, 12 publications were found to report indistinguishable phenotypes between $CD19^{Cre/WT}$ and $CD19^{WT/WT}$. Seven articles indicated effects of CD19-Cre allele to B cell function and/or disease development or progression in mice. It is possible that the effects of hypomorphic CD19 expression are additionally influenced by the genetic background, explaining for the variability in the reported phenotypes. However, the mixed notions on the possible role of the CD19-Cre allele in B cell function attest the need of focused examination on this topic. Further investigation is needed to understand the molecular mechanisms underlying the effects observed by us and others. The extensive utilization of the CD19-Cre mouse model in immunology research underscores the importance of addressing potential limitations of this mouse model.

We conclude that researchers should exercise prudence when selecting Cre driver models, as integration of the Cre cassette alone could impact B cell function and phenotype, and enhance reporting of $CD19^{WT/WT}$ control data together with $CD19^{Cre/WT}$. This caution should be equally extended to new, emerging models. To improve the low Cre-mediated deletion efficiency in CD19-Cre model, Yasuda and colleagues generated a new CD19-codon-improved Cre (iCre) model with superior recombination activity in developing B cells compared to the CD19-Cre and improved specificity compared to the Mb1-iCre[21]. However, this model also features reduced expression of CD19[21] suggesting that it may have similar limitations than those observed in our study.

Methods

Mice

The CD19-Cre mice[8,14], equivalent to the Jackson Laboratory (B6.129P2(C)-Cd19tm1(cre)Cgn/J), were maintained under specific-pathogen-free conditions. All experiments were done with age- (8–12 weeks), and sex-matched animals and WT littermate controls ($CD19^{WT/WT}$) were used. All animal experiments were approved by the Ethical Committee for Animal Experimentation in Finland (62/2006; animal license numbers: KEK/2018-2504-Mattila, ESAVI/24,046/2021 and ESAVI/24,947/2024) and carried out in accordance with the Finnish Act on Animal Experimentation. The ARRIVE guidelines have been followed for conducting and reporting animal experiments.

Immunisations

At the age of 8–10 weeks, groups of WT ($CD19^{WT/WT}$) and CD19-Cre ($CD19^{WT/Cre}$) mice were immunised (i.p.) with 50 µg of NP_{31}-KLH in 150 µl of Imject Alum-PBS (N-5060, Biosearch Technologies) or 50 µg of NP-Ficoll in 150 µl of PBS for T-dependent (TD) or T-independent (TI) immunisation, respectively. Blood (~ 100 µl) was sampled from lateral saphenous veins on day − 1 (preimmunisation) and every week after immunisation on days + 7, + 14, + 21, and + 28. Coagulated blood was spun at + 4 °C/2500 rpm for 10 min, and serum was collected and stored at − 20 °C.

ELISA

Total and NP-specific antibody levels were measured by ELISA on half-area 96-well plates (Greiner Bio-One, 675,061) as previously described[22].

Class-switch recombination

B cells purified from $CD19^{WT/WT}$ or $CD19^{WT/Cre}$ spleens were labelled with 5 µM of Cell Trace Violet (CTV) for 20 min at 37 °C in RPMI. Labelled B cells (10^5 per well) were incubated with LPS (5 µg/ml), IL-4 (10 ng/ml), IL-2 (20 ng/ml), IFNγ (20 ng/ml), $F(ab')_2$ anti-IgM (10 µg/ml), or a combination of those, in a 96 well U-bottom plate for 3 days (CSR). Cells were washed, blocked with mouse Fc-block and stained as described before[22]. Samples were washed one more time and acquired on BD LSR Fortessa. Class-switch was analysed using FlowJo software (Tree Star, USA).

Phospho-flow

Isolated splenic B cells were rested for 20 min in starvation buffer (0.5% FCS in RPMI), and 4×10^6 cells in 800 µl of starvation were stimulated with 10 µg/ml of $F(ab)_2$ goat anti-mouse IgM antibodies in solution for 15 min. After activation, B cells were instantly fixed with 4% PFA for 10 min at room temperature (RT). Samples were split in a V-bottom 96-well plate at a concentration of 2×10^6 cells per ml and washed with 1% BSA in PBS. Fixed cells were stained with primary antibodies and Fc block in permeabilization buffer (0.5% FCS, 0.05% Triton-X in PBS) for 1 h at room temperature. Samples were washed twice with 1% BSA in PBS and secondary antibodies were incubated for 1 h at RT. Samples were washed again twice with 1% BSA in PBS. Cells were then resuspended again in 1%BSA in PBS and analysed by flow cytometry, on BD LSR Fortessa. The following antibodies were used: phospho-Akt (Ser473) (4058, Cell Signalling), AlexaFluor 647 mouse anti-Btk (pY223)/Itk (pY180) (558,507, BD Biosciences), phospho-p44/42 MAPK (Erk1/2) (Thr202/Tyr204) rabbit Ab (9101, Cell Signalling), phospho-PI3 kinase p85 (Tyr458)/p55 (Tyr199) rabbit Ab (4228, Cell Signalling), phospho-S6 ribosomal protein (Ser235/236) rabbit mAb (4856, Cell Signalling), Alexa Fluor 488 mouse anti-PLCγ2 (pY759) (558,507, BD Biosciences), Alexa Fluor 488 donkey anti-rabbit IgG (H + L) (A21206, Invitrogen) and purified rat anti-mouse CD16/CD32 (553,142, BD Biosciences). Samples were analysed using FlowJo software (Tree Star, USA).

Phospho-flow in MZ and B1a cells

Isolated splenocytes and peritoneal cells were rested for 20 min in starvation buffer (0.5% FCS in RPMI), and 9×10^6 cells per condition were stimulated with 10 µg/ml of $F(ab)_2$ goat anti-mouse IgM antibodies in solution for 15 min. After activation, samples were cold centrifuged and split in a V-bottom 96-well plate at

a concentration of 2×10^6 cells per ml. Cells were incubated with mouse Fc-block and eBioscience™ Fixable Viability Dye eFluor™ 780 (65-0865-14, Thermo Fisher) in MACS buffer (0.5% BSA and 2 mM EDTA in PBS) for 10 min on ice. Samples were washed twice with MACS buffer and stained with appropriate extracellular markers for 15 min on ice: BD Pharmingen™ PerCP-Cy™5.5 Rat Anti-Mouse CD45 (550,994, BD Biosciences), Alexa Fluor® 647 anti-mouse IgD Antibody (405,708, Biolegend), BD Horizon™ V450 rat anti-mouse IgM (560,575, BD Biosciences), CD93 (AA4.1) monoclonal antibody, PE-Cyanine7 (25-5892-81, eBioscience), BD Horizon™ BV510 rat anti-mouse CD23 (563,200, BD Biosciences), anti-mouse/human CD45R/B220 (Alexa Fluor® 647) (103,226, BioLegend) and CD5 monoclonal antibody (53–7.3), PE, eBioscience™ (12-0051-82, e-Bioscience). Stained cells were washed twice with MACS buffer and fixed with 1% PFA for 10 min at room temperature on ice. Fixed cells were permeablized (2% FCS and 0.05% Saponin in PBS) for 10 min on ice and incubated with AlexaFluor 488 mouse Anti-Btk (pY223)/Itk (pY180) (564,847, BD Biosciences) and Alexa Fluor 488 mouse anti-PLCγ2 (pY759) (558,507, BD Biosciences) for 30 min on ice. Samples were washed twice with MACS buffer and analysed by flow cytometry, on BD LSR Fortessa, and FlowJo software (Tree Star, USA).

Statistics

Statistical significance was calculated using unpaired or paired Student's t-test assuming a normal distribution of the data. Statistical values are denoted as: $^*P < 0.05$, $^{**}P < 0.01$, $^{***}P < 0.001$. Graphs were created in GraphPad Prism 9.

Availability of data and materials

The raw data supporting the conclusions of this article is available by request from the corresponding author (P.K.M.).

Received: 6 March 2024; Accepted: 18 December 2024
Published online: 08 January 2025

References

1. Hobeika, E. et al. Testing gene function early in the B cell lineage in mb1-cre mice. *Proc. Natl. Acad. Sci. U S A.* **103**(37), 13789–13794. https://doi.org/10.1073/PNAS.0605944103/ASSET/76D3E661-70EB-4484-BE16-26F4884BB6AC/ASSETS/GRAPHIC/ZPQ0350633370006.JPEG (2006).
2. Kraus, M., Alimzhanov, M. B., Rajewsky, N. & Rajewsky, K. Survival of resting mature B lymphocytes depends on BCR signaling via the Igα/β heterodimer. *Cell.* **117**(6), 787–800. https://doi.org/10.1016/J.CELL.2004.05.014 (2004).
3. Rickert, R. C., Roes, J. & Rajewsky, K. B lymphocyte-specific, cre-mediated mutagenesis in mice. *Nucleic Acids Res.* **25**(6), 1317–1318. https://doi.org/10.1093/nar/25.6.1317 (1997).
4. Victoratos, P. et al. FDC-specific functions of p55TNFR and IKK2 in the development of FDC networks and of antibody responses. *Immunity.* **24**(1), 65–77. https://doi.org/10.1016/j.immuni.2005.11.013 (2006).
5. Hussain, R. Z. et al. α4-integrin deficiency in B cells does not affect disease in a T-cell-mediated EAE disease model. *Neurol Neuroimmunol. Neuroinflamm.* https://doi.org/10.1212/NXI.0000000000000563 (2019).
6. Pasqualucci, L. & Klein, U. Mouse models in the study of mature B-cell malignancies. *Cold Spring Harb Perspect Med.* https://doi.org/10.1101/CSHPERSPECT.A034827 (2021).
7. Srinivas, S. et al. Cre reporter strains produced by targeted insertion of EYFP and ECFP into the ROSA26 locus. *BMC Dev. Biol.* **1**, 1–8. https://doi.org/10.1186/1471-213X-1-4 (2001).
8. Mattila, P. K. et al. The actin and tetraspanin networks organize receptor nanoclusters to regulate B cell receptor-mediated signaling. *Immunity.* **38**(3), 461–474. https://doi.org/10.1016/j.immuni.2012.11.019 (2013).
9. Zhao, Y. et al. Altered phenotype and enhanced antibody-producing ability of peripheral B cells in mice with Cd19-driven cre expression. *Cells.* https://doi.org/10.3390/CELLS11040700 (2022).
10. Depoil, D. et al. CD19 is essential for B cell activation by promoting B cell receptor-antigen microcluster formation in response to membrane-bound ligand. *Nat. Immunol.* **9**(1), 63–72. https://doi.org/10.1038/NI1547 (2008).
11. Conley, M. E. et al. Primary B cell immunodeficiencies: Comparisons and contrasts. *Annu. Rev. Immunol.* **27**, 199–227. https://doi.org/10.1146/ANNUREV.IMMUNOL.021908.132649 (2009).
12. Engel, P. et al. Abnormal B lymphocyte development, activation, and differentiation in mice that lack or overexpress the CD19 signal transduction molecule. *Immunity.* **3**(1), 39–50. https://doi.org/10.1016/1074-7613(95)90157-4 (1995).
13. Fujimoto, M. & Sato, S. B cell signaling and autoimmune diseases: CD19/CD22 loop as a B cell signaling device to regulate the balance of autoimmunity. *J. Dermatol. Sci.* **46**(1), 1–9. https://doi.org/10.1016/j.jdermsci.2006.12.004 (2007).
14. Rickert, R. C., Rajewsky, K. & Roes, J. Impairment of T-cell-dependent B-cell responses and B-l cell development in CD19-deficient mice. *Nature.* **376**(6538), 352–355. https://doi.org/10.1038/376352A0 (1995).
15. Tedder, T. F. CD19: A promising B cell target for rheumatoid arthritis. *Nat. Rev. Rheumatol.* **5**(10), 572–577. https://doi.org/10.1038/NRRHEUM.2009.184 (2009).
16. van Zelm, M. C. et al. An antibody-deficiency syndrome due to mutations in the CD19 gene. *N. Engl. J. Med.* **354**(18), 1901–1912. https://doi.org/10.1056/NEJMOA051568 (2006).
17. Mattila, P. K., Batista, F. D. & Treanor, B. Dynamics of the actin cytoskeleton mediates receptor cross talk: An emerging concept in tuning receptor signaling. *J. Cell Biol.* **212**(3), 267–280. https://doi.org/10.1083/jcb.201504137 (2016).
18. Wang, Y. et al. The physiologic role of CD19 cytoplasmic tyrosines. *Immunity.* **17**(4), 501–514. https://doi.org/10.1016/S1074-7613(02)00426-0 (2002).
19. Sato, S., Miller, A. S., Howard, M. C. & Tedder, T. F. Regulation of B lymphocyte development and activation by the CD19/CD21/CD81/Leu 13 complex requires the cytoplasmic domain of CD19. *J. Immunol.* **159**(7), 3278–3287 (1997).
20. Fearon, D. T. & Carroll, M. C. Regulation of B lymphocyte responses to foreign and self-antigens by the CD19/CD21 complex. *Annu. Rev. Immunol.* **18**, 393–422. https://doi.org/10.1146/ANNUREV.IMMUNOL.18.1.393 (2000).
21. Yasuda, T. et al. Generation and characterization of CD19-iCre mice as a tool for efficient and specific conditional gene targeting in B cells. *Sci. Rep.* https://doi.org/10.1038/S41598-021-84786-6 (2021).
22. Sarapulov, A. V. et al. Missing-in-metastasis/metastasis suppressor 1 regulates B cell receptor signaling, B cell metabolic potential, and T cell-independent immune responses. *Front Immunol.* **11**(April), 1–20. https://doi.org/10.3389/fimmu.2020.00599 (2020).

Acknowledgements

We are thankful to Laura Grönfors, M. Özge Balci and Chiara Urban for technical assistance. Turku Bioscience

Cell Imaging and Cytometry Core and Biocenter Finland are acknowledged for providing research infrastructures. This work was supported by the Research Council of Finland's Flagship InFLAMES (decision numbers: 337530 and 357910) and project funding (decision numbers: 296684, 327378, and 339810 to P.K.M.), and the Sigrid Jusélius (to P.K.M.) and Finnish Cultural Foundations (D.M.C. and S.H-P).

Author contributions

Conceptualization, S.H-P & P.K.M.; Methodology, D.M.C., S.H-P & P.K.M.; Validation, D.M.C., S.H-P; Formal Analysis, D.M.C., S.H-P.; Investigation, D.M.C., S.H-P.; Resources: P.K.M.; Data Curation, D.M.C., S.H-P. and P.K.M.; Writing—Original Draft Preparation, S.H-P, P.K.M.; Writing—Review and Editing, D.M.C., S.H-P., P.K.M.; Visualization, D.M.C., S.H-P & P.K.M; Supervision, S.H-P. and P.K.M.; Project Administration: P.K.M.; Funding Acquisition: P.K.M. All authors have read and agreed to the published version of the manuscript.

Declarations

Competing interests

The authors declare no competing financial and/or non-financial.

Additional information

Supplementary Information The online version contains supplementary material available at https://doi.org/10.1038/s41598-024-83954-8.

Correspondence and requests for materials should be addressed to P.K.M.

Reprints and permissions information is available at www.nature.com/reprints.

Publisher's note Springer Nature remains neutral with regard to jurisdictional claims in published maps and institutional affiliations.